JOURNAL OF CULTURAL ANALYSIS AND SOCIAL CHANGE

Journal of Cultural Analysis and Social Change,
2025, 10(3), 1114-1122
ISSN: 2589-1316

Sabo Dam Capacity Modelling Based on Its Performance Index

Shakti Rahadiansyah[1], Lily Montarcih Limantara[2*], M. Bisri[3], Tri Budi Prayogo[4]

[1]*Doctoral Program in Department of Water Resources, Faculty of Engineering, University Brawijaya, INDONESIA.*
[2] *Department of Water Resources, Faculty of Engineering, University Brawijaya, INDONESIA*

*Corresponding Author: lilymont@ub.ac.id

Citation: Rahadiansyah, S., Limantara, L. M. Bisri, M. and Prayogo, T. B. (2025). Sabo Dam Capacity Modelling Based on Its Performance Index, *Journal of Cultural Analysis and Social Change*, 10(3), 1114-1122. https://doi.org/10.64753/jcasc.v10i3.2566

Published: November 29, 2025

ABSTRACT

Capacity determined the advantage of a sabo dam in volcanic disaster management. By this research, the capacity function can be approached by infrastructure performance indexing. Its data are derived from eighty-five sabo dams that are installed in Mount Merapi in Java Island - Indonesia, and there is consisting of fifteen river system with upstream connected to its crater, i.e., Apu, Pabelan, Trising, Krasak, Blongkeng, Batang, Bebeng, Putih, Lamat, Senowo, Boyong, Kuning, Opak, Gendol, and Woro. The methodology is consisted of three steps of SEM PLS analysis for selecting the adequate indicators, followed by correlation analysis to improve the retained ruling indicators and generalized reducing gradient to obtain the weight of each indicator. The indicators of capacity modeling are arranged in three aspects as IC = 0.73F+0.07R+0.30S consecutively F is for physical, R is for regulative, and S is social aspect. The t-test shows the strong correlation valued as $t = 0.05 < t$ table = 1.29 means sabo dam capacity are dependable on nineteen indicators of: Spillway (f11), Main dam (f12), Wings (f13), Drip hole (f14), Sub dam (f15), Apron (f16), Apron's wall (f17), Side dyke's heap (f18), Dyke's wall (f19), Dyke's frame (f110), Dyke's top (f111), Depth (f35), and Sabo dam capacity (f41) gathered in physical aspect, then Technical Recommendation (r23) in regulative aspect and social aspect including Occupation (s11), Economic (s12), Education (s13), Private share (s22) and Livestock (s34).

Keywords: Model, Lahar Capacity, SEM-PLS, Correlation, GRG

INTRODUCTION

Located within the Pacific Ring of Fire and at the intersection of three converging tectonic plates, Indonesia is highly susceptible to natural disasters (Prasetyo et.al, 2023). The tectonic and volcanic activities, along with their associated hazards (Iskandar et.al, 2022) such as volcanic eruptions, lahar floods (Solikhina et.al, 2015), earthquakes, and tsunamis, are frequent and persistent occurrences. Sabo dams play a vital role as protective infrastructure against volcanic disasters, and their effectiveness depends on accurate capacity assessment (Chen et.al, 2016). The numerous approaches have been employed in previous studies to estimate the capacity of sabo dams (Kim et.al, 2017). From a geometrical perspective (Rashak and Khassaf, 2020; Jarwoto and Azizul Hakim, 2021), three primary parameters—river width, dam height, and riverbed slope—serve as the foundational elements in such estimations (Horiguchi and Richefeu, 2020). Acquiring this data typically involves field surveys, although remote sensing imagery may also be utilized, provided that necessary correction and validation steps are carried out (Park et.al, 2024).

In Indonesia, several approaches have been initiated to measure the performance of sabo dams (Kholiq, 2017). As a volcanic archipelago, the government bears the responsibility of formulating regulations to guide the estimation of sabo dam performance. In this context, "performance" is defined broadly and varies depending on its intended application—ranging (Aweez et.al, 2021, Sajid and Naji, 2021) from prioritization of funding, operation and maintenance, emergency response planning, to technical evaluation. However, in terms of capacity, few estimation methods have been developed based on the rapid assessments, which are usually dominated by geometric formulas.

Balai Teknik Sabo under the Ministry of Public Works emphasizes a physical-condition-based approach to assessing the sabo dam performance. This method uses the relative index values to represent the structural condition of sabo dam components. The framework comprises four main groups to comprehensively evaluate the dam's condition: the main dam structure, embankments, reinforcements, and other attributive components. Components such as the main dam body, sub-dams, spillways, the presence of vegetation, and inspection ladders are surveyed to estimate the dam’s performance level. However, this method is often criticized for focusing too heavily on the physical aspects, which do not capture the full spectrum of sabo dam performance, particularly excluding non-physical factors. Elements such as human behavior in the surrounding area, spatial planning, and policy implementation are believed to have significant, though indirect, impacts on the dam’s functionality during disasters (Gerhana et.al, 2023). A study by Purwantoro et.al (2020) attempts to map all potentially influential factors in sabo dam performance. To better understand non-technical aspects, this framework gathers all possible contributing elements, tests relationships among variables, analyzes trends, and draws the conclusions through various statistical methods.

The physical aspects examined in the study go beyond infrastructure to include the riparian conditions such as vegetation, river bends, and the shape of riverbeds and banks (Ma et.al, 2013). Meanwhile, the non-physical aspects encompass regulatory and social factors that influence spatial implementation and socio-human conditions that are affecting the dam (Lyu et.al, 2024). The study also effectively assigns weight to the relative contributions of physical, regulatory, and social aspects that are representing them with a relative index scale from 0 to 5 to indicate the sabo dam performance. These index scores need further development to allow more practical use, such as estimating actual characteristics of sabo dams.

The examples of such applications include construction cost estimation, predicted post-construction river gradient, protected areas, capacity, and legal mining limits. To achieve the accurate capacity estimation, several steps are proposed. The first step involves testing the alignment of variables by using a structural mathematical model that includes capacity as a new factor. This analysis identifies which factors remain relevant and which must be removed, necessitating modifications to Purwantoro’s original framework. The second step is conducting the correlation analysis among dominant variables to identify those with the strongest influence on the capacity estimation model. Eliminating weaker variables is crucial for simplifying the framework and enabling faster yet accurate performance estimation, especially in urgent scenarios. The third step is reassigning weights to the physical, regulatory, and social aspects after incorporating the capacity variable. By using the Generalized Reduced Gradient (GRG) method, the selected variables—based on the field data—are iteratively interpolated to minimize the deviation from the average index value.

As a result, the weights for physical, regulatory, and social aspects (initially 0.67, 0.27, and 0.10, respectively (Gerhana et.al, 2024) are adjusted. This step affects not only the physical aspect, where capacity is integrated, but also the regulatory and social aspects and their respective components and indicators. The final step is formulating the index values that correspond to the actual capacity of the sabo dam, ensuring the internal consistency among them. By adjusting the variables such as river width, dam height, and riverbed slope, the absolute value of the dam's capacity can be estimated. A regression-based approach is used to improve precision, including by adding constant values to the enhance formula accuracy. The statistical tests of t-tests are employed to validate the results (Lyu et.al, 2024). A valid formulation from this process will precisely enable the capacity estimation and support the sabo dam performance prediction in the event of disasters (Cho, 2016).

MATERIALS AND METHODS

Research Location

The study is conducted in both Central Java Province and Special Territory of Yogyakarta within Java Island Indonesia where Mount Merapi lies among two provincial administrative areas. The historical record shows that the lahar flow is dominated to the North West to south east direction (Ainia and Jirzanah, 2021; Munir, 2019) where two hundred and eighties of sabo dam installed to prevent the volcanic debris flood (Permana, 2021; Dewi et.al, 2022) threatening the Yogyakarta City, highway road accessibility, irrigation area to the heritage temples of ancient Java (Sukatja and Alfianto, 2017). The eighty-five of sabo dam, about one third of the sabo total population, are used as the samples.

Yet not all of the samples are used in the model running. Sixty-nine is actively used in the GRG running, while the remaining sixteen is used for back up, calibration, and verification. The distribution of sample sabo dam over Mount Merapi is described as follows:

1. Thirteen sabo dam in Pabelan River: PA-C Oprit (Sengi), PA-C1 (Banyudono), PA-C1a (Candi Asu), PA-C1b (Candi Pendem), PA-C1c (Candi Pendem), PA-C2 (Banyudono), PA-C5 (Kojor), PA-D0 (Candi Pendem), PA-C (Pasekan), PA-C3, PA-C4, PA-D1, and PA-D2
2. Eight sabo dam in Kuning River: KU-C (Wedo), KU-D2 (Grogol), KU-RC3, KU-D1, KU-C1a, KU-C Wedomartani, KU-C Purwomartani, and KU-D3 Pantiasih.
3. Eight sabo dam in Boyong River: BO-D3, BO-D4 (Kemiri), BO-D6, BO-D7, BO-C5, BO-C6, BO-C7 Kemput, and BO-C1a Wonorejo.
4. Seven sabo dam in Bebeng River: BE-C4, BE-C9, BE-C10, BE-D4, BE-D5, BE-D8, BE-RD2.
5. One sabo dam in Opak River: OP-C (Pagerjurang)
6. One sabo dam in Senowo River: SE-RD5
7. Six sabo dam in Lamat River: LA-D1, LA-D2 (Sumber), LA-D3 (Gendungan), LA-D0 (Gemer), LA-C6 (Musuk), LA-D3 (SumberKB).
8. Twelve sabo dam in Gendol River: GE-C (Jambon), GE-C Rogobangsan, GE-C Jerukan, GE-C (Bronggang), GE-C 10, GE-C (Karanglo), GE - D5, GE-C(Plumbon), GE-C7(Morangan), GE-C12, GE-D2, GE-D1.
9. Nine sabo dam in Krasak River: KR-C (Blaburan), KR-C (Gedoyo), KR-C (Kembang), KR-C3 (Kranggan), KR-D3 (Gondoarum), KR-C0 (Lumbungrejo), KR-C (Blaburan), KR-D1 (Kranggan), KR-D5 (Tunggul Arum)
10. Four sabo dam in Trising River: TR-RD1, TR-C8 (Sengi), TR-D4 (Sengi), TR-R4
11. Nineteen sabo dam in Putih River: PU-D1 (Mranggen), PU-C2, PU-C13, PU-D3, PU-D4, PU-D5, PU-RD2, PU-C10 (Ngepos), PU-C11/12 (Gremeng), PU-RD1, PU-C8, PU-C8A, PU-RRC3, PU-C11, PU-C (Seloiring).
12. Five sabo dam in Apu River: AP-D2, AP-D3, AP-D4, AP-RD1a, AP-RD2.

Figure1 Presents the Sabo Dam Distributions Over Mount Merapi.

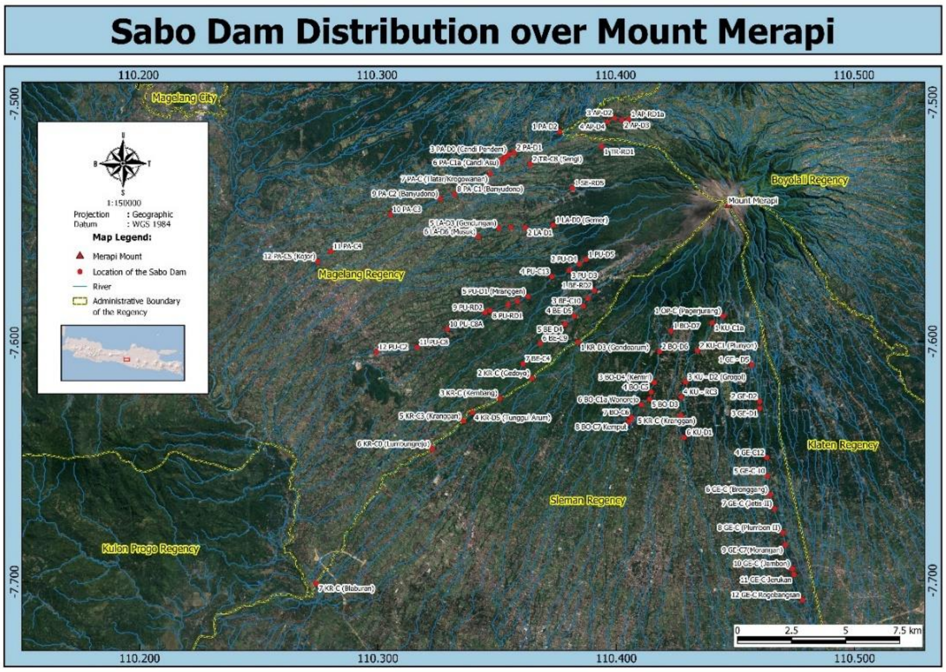

Figure 1 Sabo Dam Distribution over Mount Merapi

Methodology

The methodology of the study is built based on the study by Purwantoro et.al (2020) and Rahadiansyah et.al (2024, 2025). The result of sabo dam field survey by Purwantoro et.al (2020) had been used as the base line of the model. It comprised of six level of qualification that is expressing the actual sabo dam condition (0-5), where zero (0) as the completely deteriorated condition and five/ 5 as the best functioned indicators. The study produces the sabo dam performance index model. Rahadiansyah et.al (2024) is adopting the capacity indicators into the model in order to further improvement as sabo dam capacity model. The correlation of indicators is then enhanced through the Rahadiansyah et.al (2025) by defining which is truly related to the capacity model. The result shows that nineteen indicators are significantly ruled over the sabo dam capacity model. Figure 2 below shows the selection of indicators that are used in the sabo dam capacity model.

Model Weighting Using GRG

The Generalized Reduced Gradient (GRG) method is used to obtain the coefficient values of all identified sabo dam capacity indicators. This method is an algorithm designed to solve both nonlinear programming problems (Zamanifar and Hartmann, 2020) and multivariable linear programming problems within a general structural framework (Trimartinni et.al, 2025). Furthermore, this method is capable of solving the multivariable linear programming problems that are involving more than one variable (Tateishi et.al, 2020). The basic formulation is as follows:

minimize f(X)

$g_i(X) = 0, i = 1….m$

$l_i \leq Xi \leq ui, i = 1…, n$

where X is a vector of *n*, ui and li are the upper and lower bounds respectively, with ui > li. If it is assumed that m < n, then generally m ≥ n implies either an infeasible problem or a unique solution. The formulations [1] through [3] represent the general form, since inequalities can be transformed into equalities as shown in Equation [2] by adding slack variables. The vector X contains the components of both the original decision variables and the slack variables. Figure 2 presents the indicator reduction form Purwantoro et.al (15) to Rahadiansyah et.al (2024, 2025)

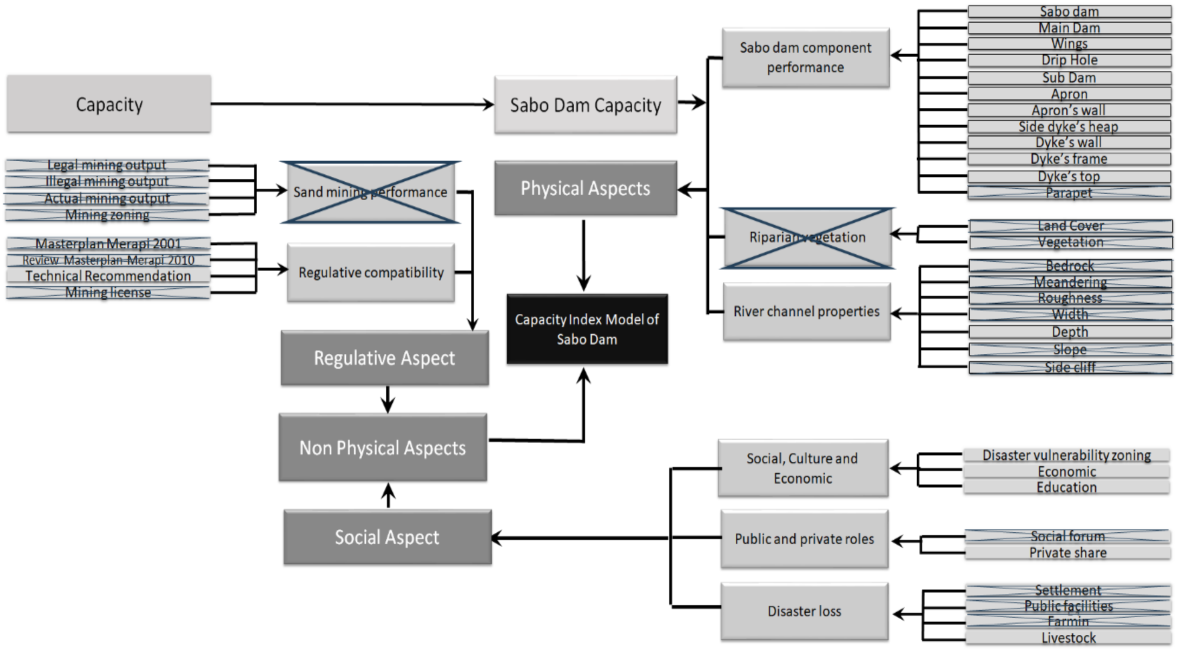

Figure 2 The Indicator Reduction form Purwantoro et.al (2020) to Rahadiansyah et.al (2024, 2025)

The fundamental idea of the GRG method is the use of Equation [2] to represent m variables, referred to as basic variables, within the framework of the remaining n – m non-basic variables. This approach is similar to the operational concept of the Simplex Method in linear programming (Pentewati et.al, 2024). If $\dot{X}$ is a feasible point, and y denotes the vector of basic variables while x represents the non-basic variables at $\dot{X}$, then X can be expressed as:

$X = (y,x), (\dot{X}) = (\dot{y}, \dot{x})$

$g(y,x) = 0$

$g = (g_1…, gm)$

It is assumed that the objective function *f* and the constraint functions g_i are differentiable. To ensure that the Equation [5] has a solution *y(x)* for all *x* within a vicinity of $\dot{x}$, the Implicit Function Theorem implies that it is sufficient for the *m x m* basis matrix $\partial g/\partial y$, evaluated at $\dot{X}$, to be non-singular. Under this assumption, the objective function can then be expressed solely as a function of x, as follows:

$F(x) = f(y(x), x)$

Thus, the nonlinear program is transformed, for *x* close to $\dot{x}$, into a simpler problem where the upper and lower bounds are only defined as:

minimize F(x)

$l_{NB} \leq x \leq u_{NB}$

with l_{NB} and u_{NB} are vectors that are representing the lower and upper bounds of *x*. The GRG method solves the original problem that is defined in Equations [1] to [3] by addressing a sequence of problems as defined in

Equations [8] and [9]. Several problems can be solved through the simple modifications of unconstrained minimization algorithms. For the sabo dam capacity model, several constrains are used as follows:

$0 \leq CI \leq 5$, capacity index – sabo dam capacity performance,
$0 \leq CI_{physical} \leq 5$, physical component in capacity index,
$0 \leq CI_{regulative} \leq 5$, regulative component in capacity index,
$0 \leq CI_{social} \leq 5$, social component in capacity index,
$\alpha \geq 0$, weight of physical component,
$\beta \geq 0$, weight of regulative component, and
$\delta \geq 0$, weight of social component.

RESULTS AND DISCUSSION

Model Result Accuracy

The model result is executed by using Microsoft Excell Solver that is producing the value with the minimum average error of all samples. It is the most optimum value among physical, regulative and social post capacity adoption. The model accuracy can be determined by the comparison of calculation and its actual value. The difference is a relative error that shows the gap among the model run and the median value of sabo dam sample. As it can be seen in Table 1, all sabo dam samples relative error is below determined $\alpha = 10\%$. The highest relative error occurred in sabo dam PU-RD2 with 4.74%. By this result it can be concluded that the model has a good accuracy and all of its result not exceed than determined error (α).

Table 1. Calibration of the sabo dam model

No.	Sabo Dam Sample	Relative Error	Capacity Index (CI)	No.	Sabo Dam Sample	Relative Error	Capacity Index (CI)	No.	Sabo Dam Sample	Capacity Index (CI)	Relative Error
1	BO-D3	0.0112	2.6058	24	PU-D5	0.0010	2.4681	47	GE-C (Bronggang)	2.5448	0.0020
2	BO-D4 (Kemiri)	0.0100	2.4000	25	PU-RD2	0.0474	2.2822	48	GE-C 10	2.5406	0.0016
3	BO-D6	0.0119	2.3910	26	KU-D3 Pantiasih	0.0088	2.4061	49	GE-C (Karanglo)	2.5406	0.0016
4	BO-D7	0.0014	2.4632	27	KR-C (Blaburan)	0.0020	2.5449	50	GE - D5	2.4970	0.0000
5	BO-C5	0.0001	2.4926	28	KU - RC3	0.0005	2.5224	51	GE-C(Plumbon)	2.5450	0.0020
6	BO-C6	0.0003	2.4820	29	KU-D1	0.0056	2.4250	52	GE-C7(Morangan)	2.5317	0.0010
7	BO-C7 Kemput	0.0016	2.5394	30	KU-C1a	0.0342	2.3150	53	GE-C12	2.5680	0.0046
8	BO-C1a Wonorejo	0.0019	2.4564	31	KR-D1 (Kranggan)	0.0153	2.6239	54	GE-D2	2.3600	0.0196
9	GE-C (Jambon)	0.0044	2.4339	32	KR-D5 (Tunggul Arum)	0.0030	2.5547	55	GE-D1	2.5845	0.0071
10	AP-D2	0.0009	2.5301	33	OP-C (Pagerjurang)	0.0397	2.6993	56	KR-C (Kembang)	2.3995	0.0101
11	AP-D3	0.0000	2.5013	34	PA-C1 (Banyudono)	0.0201	2.6419	57	KR-C3 (Kranggan)	2.3018	0.0393
12	AP-D4	0.0000	2.4975	35	PA-C1a (Candi Asu)	0.0024	2.4514	58	KR-D3 (Gondoarum)	2.4420	0.0034
13	AP-RD1a	0.0014	2.5368	36	PU-D5	0.0010	2.4681	59	KR-C0 (Lumbungrejo)	2.6492	0.0223
14	AP-RD2	0.0085	2.5923	37	PA-C1c (Candi Pendem)	0.0045	2.4333	60	LA-D1	2.3670	0.0177
15	BE-C4	0.0004	2.4810	38	PA-C2 (Banyudono)	0.0018	2.5426	61	LA-D2 (Sumber)	2.3675	0.0176
16	BE-C9	0.0055	2.5744	39	PA-C5 (Kojor)	0.0032	2.5564	62	LA-D3 (Gendungan)	2.5026	0.0000
17	BE-C10	0.0001	2.5109	40	PA-DO (Candi Pendem)	0.0143	2.3806	63	LA-DO (Gemer)	2.6130	0.0128
18	BE-D4	0.0000	2.5028	41	PA-C (Pasekan)	0.0060	2.4229	64	LA-D6 (Musuk)	2.5123	0.0002
19	BE-D5	0.0001	2.4884	42	PU-D1 (Mranggen)	0.0127	2.6127	65	LA - D3 (SumberKB)	2.5001	0.0000
20	BE-D8	0.0000	2.4935	43	PU-C2	0.0163	2.3722	66	PA-C3	2.5316	0.0010
21	BE-RD2	0.0005	2.5217	44	PU-C13	0.0152	2.6232	67	PA-C4	2.5435	0.0019
22	KR-C (B1br)	0.0027	2.4476	45	PU-D3	0.0019	2.4565	68	PA-D1	2.5402	0.0016

23	KR-C (Bedoyo)	0.0010	2.5322	46	PU-D4	0.0010	2.4687	69	PA-D2	2.4268	0.0054

As the model are built up on three hierarchical structures of aspect (physical F – regulative R – social S), variables (sabo dam component F_1, river channel properties F_3, capacity F_4, regulative compatibility R_2, social culture and economic S_1, public private role S_2, disaster loss S_3), and nineteen indicators, the result of all parameters are presented in Table 2 as follows. Furthermore Figure 3 shows the comparison of variables in radar diagram. Both are presenting the weight among three aspects, relative weight of the seven variables, and the magnitude comparison of nineteen indicators. In order to set a validation of the capacity model result, the t-test are chosen as the statistical validation method.

Table 2. Parameters Weight and Magnitude

Aspect		Indicator			
F	0.728486141	f11	0.74085	f35	1.25198
R	0.069101432	f12	1.23973	f41	6.32985
S	0.202412427	f13	0.50941	r23	0.40530
Variable		f14	1.15970	s11	0.03285
F1	0.584268	f15	2.15560	s12	0.33736
F3	0.167755	f16	0.07430	s13	0.06794
F4	0.247977	f17	0.32980	s22	0.04343
R2	1.000000	f18	0.36416	s34	0.12666
S1	0.517897	f19	0.69695		
S2	0.184468	f110	0.53589		
S3	0.297635	f111	0.68671		

As seen in Figure 3, the variable of regulative compatibility has only one indicator i.e., technical recommendation. This condition resulting is in undivided full scale of 1.00 point. While other variable of physical and social has to share with others such as physical aspect (F) for three variables and so with social (S) aspect covering three variables of S_1, S_2, and S_3.

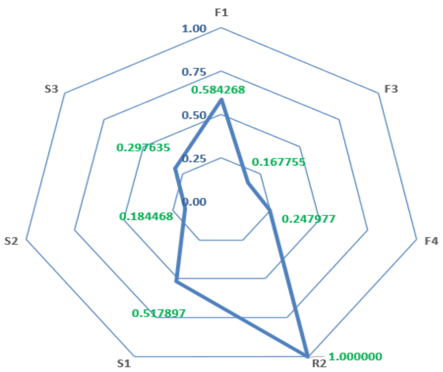

Figure 3 the Variables Weight Result

Validation by t-test

The two-way t-test is used to validate sabo dam capacity model by comparing t value of both calculation and table. This method will be produced a value within distribution curve. The value will determine the inter parameter influence (May, 2025). The t values within H_0 rejection area will show the existence of inter parameter correlation. In the opposite t calculation value within H_0 acceptance area will show no correlation of the parameters (Lajan and Al-Barzinji, 2022; Zina and Al Aubydi, 2022). Table 3 shows the calculation of sabo dam capacity model. By the result it can be concluded that t dataset (calculation) is lower than t-table and located in H_0 rejection area.

Table 3. Validation using t-test

Statistical Properties	Calculation
S^2	0.0072
S	0.0846662
t dataset (calculation)	0.058899
df	68
α	0.1
α tale reading (two side)	0.2
Average Relative Error	0.0072
t table	1.29

CONCLUSION

The sabo dam capacity determines the benefit of a sabo dam during the event of a volcanic disaster. By the adoption of capacity indicator, the number of significant indicators is changing. It's reducing from forty to twenty-seven then twenty-five with different indicators sustain and then nineteen. The addition of capacity indicators is changing the compatibility of aspect, variable, and indicator to the more suitable for capacity.

Several variables that are eliminated during SEM PLS stage and correlation analysis show actual validation of the capacity indicator adoption. Riparian vegetation (F_2), and Sand mining performance (R_1) shows incompatibility with the capacity indicator (f_{41}) by eliminating in capacity model. The reason for F_2 to be incompatible is that vegetation by cover and type of species indeed not adding or reducing the actual sabo dam capacity. It may help to retain lahar flow within the river body by creating side resistance, but it does not add some additional capacity. Furthermore, for the R_1 that the sand mining activities in Mount Merapi is dominated by illegal parties, therefore it is losing the correlation with the actual sabo dam capacity. The weakness of the sand mining management implementation crates no longer reliable number with the field finding of sabo dam capacity.

The final result of sabo dam capacity model $IC = 0.73F+0.07R+0.30S$ is changing the previous sabo dam performance model of $IL = 0.63F + 0.27R + 0.10S$. In the matter of capacity, the influence of physical is increasing while the unreliable regulative aspect is decreasing. The social aspect that may be generating the public needs to influence the sabo dam through agriculture, tourism, sand exploration is carried out around volcanic disaster mitigation infrastructure. Validation through t-test shows that rejection of H0 concludes the correlation of the aspect, variable, and indicator of the model and ensuring the validity and robustness of the model.

REFERENCES

Aweez, Sh.J., Darwesh, D.A., and Othman, B.A. (2021) "Application of some single and integrated index equation to assess heavy metal in different soils in erbil governorate," *Iraqi Journal of Agricultural Sciences*, 52(4), pp. 868-875. Available at: https://doi.org/10.36103/ijas.v52i4.1394

Azmeri, Kasury, A.R., Istiqfarah, Ziana, Yulianur, A., Syahreza, S., Hidayah, E., Herawati, H., and Jualiastuti. (2025) "Enhancing disaster mitigation through sediment transport modelling – Development of natural based solutions for the future," *Journal of Water and Land Development*, 66, pp. 38-46. Available at: https://doi.org/10.24425/jwld.2025.155299

Azmeri, A., Legowo, S. and Rezkyna, N. (2020) "Interphase modeling of soil erosion hazard using a Geographic Information System and the Universal Soil Loss Equation," *Journal of Chinese Soil and Water Conservation*, 51(2), pp. 65–75. Available at: https://doi.org/10.29417/JCSWC.202006

Chen, H., Cui, P., Chen, J., and Tang, J. (2026) "Effects of spillway types on debris flow trajectory and scour behind a sabo dam," *J Mt Sci*, 13(2), pp. 203–212. Available at: https://doi.org/10.1007/s11629-015-3607-6.

Cho, E. (2016) "Making reliability reliable: a systematic approach to reliability coefficients," *Organizational Research Methods*, 19(4), pp. 651–682. Available at: https://doi.org/10.1177/1094428116656239 \

Dewi, N.K., Jazaul, I., and Nursetiawan, I. (2022) "Effect of land erosion on sabo," *Jurnal Teknik Sumber Daya Air*, 2(1), pp. 25-34, Available at: https://jtsda.hathi.id/index.php/jtsda/article/view/29.

Gerhana, S.E.W., Purnomo, N.H., Mujib, M.A., M. Shofwan, and H. Mahat. (2023) "The influence of the sabo dam Bronggang on disaster mitigation public about the danger of Merapi Mountain eruption," *International Journal of Geography, Social, and Multicultural Education*, 1(1), pp. 49-57. Available at: https://journal.unesa.ac.id/index.php/ijgsme

Horiguchi, T., and Richefeu, V. (2020) "post-analysis simulation of the collapse of an open sabo dam of steel pipes subjected to boulder laden debris flow," *International Journal of Sediment Research*, 35(6), pp. 621–635. Available at: https://doi.org/10.1016/J.IJSRC.2020.05.002.

Iskandar, I., Yermadona, H., and Herista, F. (2022) "Tinjauan efektifitas check dam tipe segiempat terhadap aliran sedimen pada irigasi Lubuk Janggan Kelurahan Ngalau Kota Padang Panjang Effectiveness review of rectangular type check dam towards sediment on the irrigation of Lubuk Janggan Kelurahan Ngalau Kota Padang Panjang)," *Ensiklopedia Research and Community Service Review*, 1(2). Available at: https://doi.org/10.33559/Err.V1i2.1136

Jarwoto, J., and Azizul Hakim, E. (2021). "Analisa desain bangunan pengendali sedimen jembatan Plapar, Slahung, Ponorogo (Design analysis of sediment control structure on Plapar bridge, Slahung, Ponorogo)," *Seminar Keinsinyuran Program Studi Program Profesi Insinyur*, 1(2). Available at: https://doi.org/10.22219/Skpsppi.V2i1.4396

Kholiq, M.A. (2017) "Simulation of the flow of lava floods after the 2010 eruption of Mount Merapi on the existence of a sabo dam on the Gendol river," *Technician*, pp. 410-415. Available at: https://www.scribd.com>document

Kim, Y., Nakagawa, H., Kawaike, K., and Zhang, H. (2017) "Study on hydraulic characteristics of sabo dam with a flap structure for debris flow," *International Journal of Sediment Research*, 32(3), pp. 452–464. Available at: https://doi.org/10.1016/J.IJSRC.2017.05.001.

Lajan, S.A., and Al-Barzinji, Y.M.S. (2022) "Detection of quantitative loci correlation with growth traits in local quail using PCR-RFLP technique," *Iraqi Journal of Agricultural Sciences*, 53(1), pp. 16-26. Available at: https://doi.org/10.36103/ijas.v53i1.1501

Lyu, G., Hirooka, A., and Kiyokuni, H. (2024) "Centrifuge experiment on capture performance of open-type sabo dam with its numerical analysis," Advances *in Civil Engineering*, article ID 5506896, 12 pages. Available at: https://doi.org/10.1155/2024/5506896.

Ma, C., Hu, K.H., and Tian, M. (2013) "Comparison of debris-flow volume and activity under different formation conditions," *Natural Hazards*, 67, pp. 261-273. Available at: https://doi.org/10.1007/s11069-013-0557-6.

May, N.T. (2025) "Hybrid multi-criteria decision-making methods: combination of preference selection index method with faire un choix adequate, root assessment method, and proximity indexed value," *Engineering, Technology & Applied Science Research*, 15(1), pp.19086-19090. Available at: https://doi.org/10.48084/etasr.9325

Munir, M.D. (2019) "Bangunan sabo dam, fungsi dan potensinya sebagai bagian dari geowisata gunung api Merapi (The sabo dam building, its function and potential as part of Merapi geo-tourism)," *Jurnal Lingkungan dan Bencana Geologi*, 10(2). Available at: https://doi.org/10.34126/jlbg.v10i2.202

Park, J., Jeong, H., and Lee, J. (2024) "National disaster management and monitoring using satellite remote sensing and geo-information," *Korean J. Remote Sens.*, 40(5), pp. 813-832. Available at: https://doi.org/10.7780/kjrs.2024.40.5.2.9.

Pentewati, P., Juwono, P.T., Limantara, L.M., and Moh. Sholichin. (2024) "Performance index model of small dam in semi-arid area," *Civil Engineering Journal*, 10(8), pp. 2645-2660. Available at: https://doi.org/10.28991/CEJ-2024-010-08-014

Permana, S. (2021) "Eling lan waspodo as a local perception for "Merapi" volcanic disaster preparedness," *Journal of Indonesian Society and Culture*, 13(2). Pp. 199-205. Available at: https://doi.org/10.15294/komunitas.v13i2.27223

Prasetyo, E., Yulianti, E., and Dewi, G.C. (2023) "The effectiveness of sabo dam modular as a clean water intake weir (case study of work for Huntap Tondo raw water project)," *Journal Research of Social Science, Economics, and Management*, 3(4), pp. 1019-1041. Available at: https://doi.org/10.59141/jrssem.v3i4.582

Purwantoro, D., Limantara, L.M., Soetopo, W., and Sholichin, M. (2020) "Sabo dam infrastructure system performance index model in Mount Merapi," *Technology Reports and Kansai University*, 62(10): 6151-6164. Access key: TRKU65087810712. Available at: https://www.researchgate.net/publication/350495913_Sabo_Dam_Infrastructure_System_Performance_Index_Model_in_Mount_Merapi

Rahadiansyah, S., Limantara, L.M., and Bisri. M. (2024) "Factors, variables, and aspects sabo dam modeling capacity based on the Purwantoro sabo dam index model," *ICWRDEP-2023 IOP Conference Series: Earth and Environmental Science*, 1311, art. ID 012005. Available at: https://doi.org/10.1088/1755-1315/1311/1/012005.

Rahadiansyah, S., Limantara, L.M., Bisri, M., and Prayogo, T.B. (2025) "Correlation of factors, variables, and aspects in sabo dam capacity modeling," *Civil Engineering and Architecture*, 13(3A), pp. 2440-2451. Available at: https://doi.org/10.13189/cea.2025.131320

Rashak, B.M., and Khassaf, S.I. (2020) "Study the local scour around different shapes of single submerged groyne," *Journal of Water and Land Development*, 47, pp. 1-9. Available at: https://doi.org/10.24425/jwld.2020.135025

Sajid, R.H., and Naji, A.A. (2021) "Evaluation the performance of senior management for the extension organization in light of the total quality standards from the standards from the standpoint of agricultural extension workers in governorates of Baghdad and Diyala from Iraq," *Iraqi Journal of Agricultural Sciences*, 52(4), pp.1008-1018. Available at: https://doi.org/10.36103/ijas.v52i4.1412

Sidik, F.B., Ramadeo, M.G., Wulandari, M.D.A., Khumairo, S.Z., Nurkholijah, E., Pangestu, F.B., Fitrinova, S., and Muhlisin, H. (2024) "Determination of sand mining Prospective zones based on sediment thickness analysis using HVSR microtemor and gravity methods: a case study in Cangkringan, Sleman, Daerah Istimewa Yogyakarta," *Journal of Scientech Research and Development*, 6(1), pp. 24-42. Available at: https://doi.org/10.56670/jsrd.v6i1.272

Solikhina, A, Thouret, J.C., Gupta, A, Sayudia, D.S, Oehlerd, J.F, and Liew, S.C. (2015) "Effects and behavior of pyroclastic and lahar deposits of the 2010 Merapi Eruption based on high resolution optical imagery," 3rd International Symposium on Earthquake and Disaster Mitigation. ISEDM 2013. Elsevier. *Procedia Earth and Planetary Science*, 12, pp. 1 – 10. Available at: www.sciencedirect.com

Sukatja, C.B., and Alfianto, A. (2017) "Revitalization of sabo dam as lahar flow controller (case study in Merapi volcano area)," *Jurnal Teknik Hidraulik*, 8(1), pp. 29-42. Available at: https://doi.org/10.32679/jth.v8i1.217

Tateishi, R., Horiguchi, T., Sonoda, Y., and Ishikawa, N. (2020) "Experimental study of the woody debris trapping efficiency of a steel pipe, open sabo dam," *International Journal of Sediment Research*, 35(5), pp. 431–443. Available at: https://doi.org/10.1016/J.IJSRC.2020.03.011.

Trimartinni, A.D., Limantara, L.M., Juwono, P.T., and Siswoyo. H. (2025) "Development of performance index model for assessing the multipurpose reservoir storage capacity," *Civil Engineering and Architecture*, 13(1), pp. 105-117. Available at: https://doi.org/10.13189/cea.2025.130106

Zamanifar, M., and Hartmann, T. (2020) "Optimization-based decision-making models for disaster recovery and reconstruction planning of transportation networks," *Natural Hazards*, 104, pp. 1-25. Available at: https://doi.org/10.1007/s11069-020-04192-5

Zina, M., and Al Aubydi, M.A. (2022) "Correlation between skin microbal infection and IgE, LPS in serum with atopic dermatitis," *Iraqi Journal of Agricultural Sciences*, 53(6), pp. 1358-1367. Available at:

